Correspondence

The Second Order Scattering Fading Model With Fluctuating Line-of-Sight

Jesús López-Fernández, Gonzalo J. Anaya-López, and F. Javier López-Martínez, *Senior Member, IEEE*

***Abstract*—We present a generalization of the notoriously unwieldy second order scattering fading model, which is helpful to alleviate its mathematical complexity while providing an additional degree of freedom. This is accomplished by allowing its dominant specular component associated to line-of-sight propagation to randomly fluctuate. The statistical characterization of the newly proposed model is carried out, providing closed-form expressions for its probability and cumulative distribution functions, as well as for its generalized Laplace-domain statistics and raw moments. We exemplify how performance analysis can be done in this scenario, and discuss the role of the fading model parameters on system performance.**

***Index Terms*—Channel modeling, fading models, Rice, Rician shadowed, second order scattering.**

I. Introduction

Double-scattering fading conditions often appear in radio propagation environments like vehicular communications [1], [2], [3], unmanned aerial vehicle-enabled communications [4], backscattering systems [5], [6], indoor mobile [7], or land mobile satellite channels [8]. A family of multiple-order scattering fading channels was originally defined by Andersen [9] and formalized by Salo [10], considering a finite number of increasing-order scattering terms. Even for its simplest formulation that consists of a line-of-sight (LoS) component plus Rayleigh *and* double-Rayleigh (dR) diffuse components, referred to as second order scattering fading (SOSF) model, its mathematical complexity and potential numerical instability have limited the applicability of this otherwise useful fading model. Only recently, an alternative formulation for the SOSF model [11] provided a reasonably simpler approach that fully avoided the original numerical issues suffered by the model, and its moment generating function (MGF) was derived for the first time.

Several state-of-the-art fading models incorporate the ability to model random amplitude fluctuations of dominant specular waves associated to LoS propagation. Relevant examples include popular fading models like the pioneering Rician shadowed (RS) [12] and its generalizations [13], [14]. Fluctuating LoS models include one additional degree of freedom over the deterministic LoS models, which can be used to recreate different phenomena: (*i*) partial/total blockages of the LoS component by environmental obstacles [12]; or (*ii*) any sort of relatively-short term amplitude fluctuation in the dominant specular wave caused, for instance, by variations in the propagation condition or by fast moving scatterers [15]. Given that the SOSF model originates from a deterministic LoS formulation, it is legitimate to ask whether an alternative formulation based on fluctuating LoS is possible for this model, enabling an improved characterization of the propagation in the aforementioned scenarios. In this line, only recently, a fluctuating double-Rayleigh with line-of-sight (fdRLoS) fading model was formulated as a combination of a randomly fluctuating LoS component plus a dR diffuse one, although the first-order Rayleigh-like component also present in the original SOSF model is neglected. In this work, we define a natural generalization of the SOSF model to incorporate random fluctuations on its LoS component, for which the moniker fluctuating second order scattering fading (fSOSF) is proposed. The newly proposed model is able to capture the same propagation conditions as the baseline SOSF model, and allows to tune the amount of fluctuation suffered by the dominant component through one additional parameter. Interestingly, the addition of a new parameter for this model does not penalize its mathematical tractability, and the resulting expressions for its chief statistics have the same functional form (even simpler in some cases) as those of the original SOSF model. The applicability of the fSOSF model for performance analysis purposes is also exemplified through some illustrative examples.

Notation: $\mathbb{E}\{X\}$ and $|X|$ denote the statistical average and the modulus of the complex random variable (RV) X respectively. The RV X conditioned to Y will be denoted as $X|Y$. The symbol $\sim$ reads as *statistically distributed as*. The symbol $\stackrel{d}{=}$ reads as *equal in distribution*. A circularly symmetric normal RV X with mean μ and variance Ω is denoted as $X \sim \mathcal{N}_c(\mu, \Omega)$.

II. Physical Model

Based on the original formulation of the SOSF model introduced by Andersen [9] and Salo [10] for a point-to-point link in a single-antenna set-up, let us consider the following definition for the received signal S as

$$S = \omega_0 \sqrt{\xi} e^{j\phi} + \omega_1 G_1 + \omega_2 G_2 G_3, \tag{1}$$

where $\omega_0 e^{j\phi}$ is the dominant specular component classically associated to LoS propagation, with ω_0 being a constant value and ϕ a RV uniformly distributed in $[0, 2\pi)$. The RVs G_1, G_2 and G_3 are distributed as independent zero-mean, unit-variance complex normal variables, i.e., $G_i \sim \mathcal{N}_c(0, 1)$ for $i = 1, 2, 3$. The constant parameters ω_0, ω_1 and ω_2 act as scale weights for the LoS, Rayleigh and dR components, respectively. Now, the key novelty of the model in (1) lies on its ability to incorporate random fluctuations into the LoS similarly to state-of-the-art fading models [12], [13] through ξ, a Gamma distributed RV with unit power and real positive shape parameter m, with probability

Manuscript received 9 February 2023; revised 5 February 2024; accepted 22 March 2024. Date of publication 3 April 2024; date of current version 19 September 2024. This work was supported in part by Junta de Andalucía, the European Union and the European Fund for Regional Development FEDER under Grant P18-RT-3175 and Grant EMERGIA20-00297, in part by MCIU/AEI/10.13039/501100011033 under Grant PID2020-118139RB-I00, and in part by Universidad de Málaga and FEDER under Grant UMA20-FEDERJA-002. The review of this article was coordinated by Prof. M. Peng. *(Corresponding author: Jesús López-Fernández.)*

Jesús López-Fernández and Gonzalo J. Anaya-López are with the Communications and Signal Processing Lab, Telecommunication Research Institute (TELMA), Universidad de Málaga, 29010 Málaga, Spain (e-mail: jlf@ic.uma.es; gjal@ic.uma.es).

F. Javier López-Martínez is with the Communications and Signal Processing Lab, Telecommunication Research Institute (TELMA), Universidad de Málaga, 29010 Málaga, Spain, and also with the Department Signal Theory, Networking and Communications, University of Granada, 18071 Granada, Spain (e-mail: fjlm@ugr.es).

Digital Object Identifier 10.1109/TVT.2024.3384582

density functions (PDFs):

$$f_\xi(u) = \frac{m^m u^{m-1}}{\Gamma(m)} e^{-mu}, \tag{2}$$

where $\Gamma(\cdot)$ is the gamma function. The severity of LoS fluctuations is captured through the parameter m, being fading severity inversely proportional to this shape parameter. In the limit case of $m \to \infty$, ξ degenerates to a deterministic unitary value and the LoS fluctuation vanishes, thus collapsing into the original SOSF distribution. Besides m, the fSOSF model is completely defined by the constants ω_0, ω_1 and ω_2. Typically, an alternative set of parameters is used in the literature for the baseline SOSF model, i.e. (α, β), defined as

$$\alpha = \frac{\omega_2^2}{\omega_0^2+\omega_1^2+\omega_2^2}, \qquad \beta = \frac{\omega_0^2}{\omega_0^2+\omega_1^2+\omega_2^2}. \tag{3}$$

Assuming a normalized channel (i.e., $\mathbb{E}\{|S|^2\} = 1$) so that $\omega_0^2 + \omega_1^2 + \omega_2^2 = 1$, the parameters (α, β) are constrained to the triangle $\alpha \geq 0$, $\beta \geq 0$ and $\alpha + \beta \leq 1$.

III. Statistical Characterization

Let us define the instantaneous signal-to-noise ratio (SNR) $\gamma = \overline{\gamma}|S|^2$, where $\overline{\gamma}$ is the average SNR. The model in (1) reduces to the SOSF one [10] when conditioning to ξ. However, it is possible to find an alternative pathway to connect this model with a different underlying model in the literature, so that its mathematical formulation is simplified.

According to [11], the SOSF model can be seen as a Rician one when conditioning to $x = |G_3|^2$. This can be leveraged to formulate the fSOSF model in terms of an underlying RS one, as shown in the sequel. For the RV γ we can express:

$$\gamma = \overline{\gamma}|\omega_0\sqrt{\xi}e^{j\phi} + \omega_1 G_1 + \omega_2 G_2 G_3|^2. \tag{4}$$

Since G_3 is a complex Gaussian RV, we reformulate $G_3 = |G_3|e^{j\Psi}$, where Ψ is uniformly distributed in $[0, 2\pi)$. Because G_2 is a circularly-symmetric RV, G_2 and $G_2 e^{j\Psi}$ are equivalent in distribution, so that the following equivalence holds for γ

$$\gamma \overset{d}{=} \overline{\gamma}|\omega_0\sqrt{\xi}e^{j\phi} + \omega_1 G_1 + \omega_2 G_2 |G_3||^2. \tag{5}$$

Conditioning on $x = |G_3|^2$, define the conditioned RV γ_x as

$$\gamma_x \triangleq \overline{\gamma}|\omega_0\sqrt{\xi}e^{j\phi} + \omega_1 G_1 + \omega_2\sqrt{x} G_2|^2 \tag{6}$$

the two last terms correspond to the sum of two RVs distributed as $\mathcal{N}_c(0;\omega_1^2)$ and $\mathcal{N}_c(0;\omega_2^2 x)$, respectively. This is equivalent to one single RV distributed as $\mathcal{N}_c(0;\omega_1^2+\omega_2^2 x)$. With all these considerations, γ_x is distributed according to a squared RS RV [12] with parameters m and

$$\overline{\gamma}_x = \frac{\omega_0^2}{\omega_1^2 + x\omega_2^2} = \overline{\gamma}(1-\alpha(1-x)), \tag{7}$$

$$K_x = \omega_0^2 + \omega_1^2 + x\omega_2^2 = \frac{\beta}{1-\beta-\alpha(1-x)}. \tag{8}$$

These parameter definitions include as special case the model in [16], for $\omega_1^2 = 0$. In the following set of Lemmas, the main first-order statistics of the fSOSF distribution are introduced for the first time in the literature; these include the PDFs, cumulative distribution function (CDF), generalized moment generating function (GMGF)[1] and the moments.

Lemma 1: Let γ be an fSOSF-distributed RV with shape parameters $\{\alpha, \beta, m\}$, i.e., $\gamma \sim \mathcal{F}_{\text{SOSF}}(\alpha, \beta, m; \overline{\gamma})$. Then, the PDFs of γ is given by

$$f_\gamma(\gamma) = \int_0^\infty \frac{m^m(1+K_x)}{(m+K_x)^m \overline{\gamma}_x} e^{-\frac{1+K_x}{\overline{\gamma}_x}\gamma - x} \times {}_1F_1\left(m; 1; \frac{K_x(1+K_x)}{K_x+m}\frac{\gamma}{\overline{\gamma}_x}\right) dx, \tag{9}$$

$$f_\gamma(\gamma) = \sum_{j=0}^{m-1} \binom{m-1}{j} \frac{\gamma^{m-j-1} e^{\frac{m(1-\alpha-\beta)+\beta}{m\alpha}} \left(\frac{\beta}{m}\right)^{m-j-1}}{(\overline{\gamma})^{m-j}(m-j-1)!\alpha^{2m-j-1}} \times \sum_{r=0}^{j} \binom{j}{r} \left(\frac{-\beta}{m}\right)^{j-r} \alpha^r \times \Gamma\left(r-2m+j+2, \frac{m(1-\alpha-\beta)+\beta}{m\alpha}, \frac{\gamma}{\alpha\overline{\gamma}}\right), \tag{10}$$

for $m \in \mathbb{R}^+$ and $m \in \mathbb{Z}^+$, respectively, and where ${}_1F_1(\cdot;\cdot;\cdot)$ and $\Gamma(a,z,b) = \int_z^\infty t^{a-1}e^{-t}e^{\frac{-b}{t}}dt$ are Kummer's hypergeometric function, and a generalization of the incomplete gamma function defined in [17], respectively.

Proof: See Appendix A. □

Remark 1: By construction, the fSOSF model degenerates to either the SOSF or RS models. This can be formally proved as follows: taking the limit $m \to \infty$ in (9) in combination with Fubini's theorem, and using [18, eq. (11)], ${}_1F_1(\cdot;\cdot;\cdot)$ reduces to a modified Bessel function of the first kind and order zero, and (9) equals [11, eq. (12)]. Similarly, making $\alpha \to 0$ in (9) causes the dependence of K_x and $\overline{\gamma}_x$ on x to vanish. Hence, the integral equals one and (9) reduces to [12, eq. (3)].

Formulating the fSOSF model in terms of a conditional RS model allows to express the statistics of the former in terms of those of the latter, in an integral form similar to (9) for any arbitrary $m \in \mathbb{R}^+$. However, for the case of integer m the statistics of the fSOSF model have a much simpler form – as exemplified in (10). As reported in [19], such a restriction has a limited impact for mild/moderate fluctuations of ξ (i.e., only has relevance for low values of m). In the sequel, we will focus on the case of $m \in \mathbb{Z}^+$ for the sake of simplicity.

Lemma 2: Let $\gamma \sim \mathcal{F}_{\text{SOSF}}(\alpha, \beta, m; \overline{\gamma})$. Then, the CDF of γ is given by

$$F_\gamma(\gamma) = 1 - e^{\frac{m(1-\alpha-\beta)+\beta}{m\alpha}} \sum_{j=0}^{m-1}\sum_{r=0}^{m-j-1}\sum_{q=0}^{j} \binom{m-1}{j}\binom{j}{q} \times \frac{(-1)^{j-q}\alpha^{q-r-m+1}}{r!} \left(\frac{\gamma}{\overline{\gamma}}\right)^r \left(\frac{\beta}{m}\right)^{m-q-1} \times \Gamma\left(q-r-m+2, \frac{m(1-\alpha-\beta)+\beta}{m\alpha}, \frac{\gamma}{\alpha\overline{\gamma}}\right). \tag{11}$$

for $m \in \mathbb{Z}^+$.

Proof: See Appendix B. □

Lemma 3: Let $\gamma \sim \mathcal{F}_{\text{SOSF}}(\alpha, \beta, m; \overline{\gamma})$. Then, for $m \in \mathbb{Z}^+$ the GMGF of γ is given by

$$\mathcal{M}_\gamma^{(n)}(s) = \sum_{q=0}^{n} \binom{n}{q} \frac{(-1)^{q+1}(m-n-q)_{n-q}(m)_q}{s^{n+1}\overline{\gamma}\alpha} \times \sum_{i=0}^{n-q}\sum_{j=0}^{q}\sum_{r=0}^{m-1-n+q} \binom{n-q}{i}\binom{q}{j}\binom{m-1-n+q}{r} \times c^{n-q-i}d^{q-j}a(s)^{m-1-n+q-r}\Gamma(1+r+i+j) \times \mathrm{U}(m+q, m+q-r-i-j, b(s)). \tag{12}$$

for $m \geq n+1$, and in (13) shown at the bottom of the next page, for $m < n+1$, where $A_k(s)$ and $B_k(s)$ are the partial fraction expansion

[1]Laplace-domain statistics enable a direct generalization to multi-antenna set-ups, for the case of independent transmit or receive branches.

coefficients given by

$$A_k(s) = \sum_{l=0}^{\sigma_1-k} \frac{\binom{\sigma_1-k}{l}}{(\sigma_1-k)!}(i+j-\sigma_1+k+l+1)_{\sigma_1-k-l} \times (\sigma_2)_l(-1)^l(-a)^{i+j-\sigma_1+k+l}(b-a)^{-\sigma_2-l},$$

$$B_k(s) = \sum_{l=0}^{\sigma_2-k} \frac{\binom{\sigma_2-k}{l}}{(\sigma_2-k)!}(i+j-\sigma_2+k+l+1)_{\sigma_2-k-l} \times (\sigma_1)_l(-1)^l(-b)^{i+j-\sigma_2+k+l}(a-b)^{-\sigma_1-l}, \quad (14)$$

with $\sigma_1 = n+1-m-q$ and $\sigma_2 = m+q$, and where $\mathrm{U}(\cdot,\cdot,\cdot)$ is Tricomi's confluent hypergeometric function [20, eq. (13.1)].

Proof: See Appendix C. □

Lemma 4: Let $\gamma \sim \mathcal{F}_{\mathrm{SOSF}}(\alpha,\beta,m;\overline{\gamma})$. Then, for $m \in \mathbb{Z}^+$ the n-th moment of γ is given by

$$\mathbb{E}[\gamma^n] = (\overline{\gamma}\alpha)^n \sum_{q=0}^{n} \binom{n}{q}(-1)^{q-n}(m-n+q)_{n-q}(m)_q \times \sum_{i=0}^{n-q}\sum_{j=0}^{q} \binom{n-q}{i}\binom{q}{j} c^{n-q-i}d^{q-j}(i+j)!. \quad (15)$$

Proof: See Appendix D. □

IV. Numerical Results

In Fig. 1, we represent the PDFs of the fSOSF fading model for different values of the LoS fluctuation severity parameter m. Parameter values are $\alpha = 0.1$, $\beta = 0.7$ and $\overline{\gamma}_{\mathrm{dB}} = 3$ dB. Monte Carlo (MC) simulations are also included as a sanity check. As the fading severity of the LoS component is increased (i.e., $\downarrow m$), the probability of occurrence of low SNR values grows, as well as the variance of the distribution.

In Fig. 2 we analyze the impact of α and β on the PDFs of the fSOSF model. Two scenarios have been considered: one with low fading severity and low average SNR ($m = 20, \overline{\gamma}_{\mathrm{dB}} = 1$ dB), and another with higher fading severity and higher average SNR ($m = 1, \overline{\gamma}_{\mathrm{dB}} = 5$ dB). In the case of mild fluctuations of the LoS component, the effect of β dominates to determine the shape of the distribution, observing bell-shaped PDFss with higher β values. Conversely, the value of α becomes more influential for the left tail of the distribution. We see that lower values of α make lower SNR values more likely, which implies an overall larger fading severity.

Finally, we analyze the outage probability (OP) under fSOSF which is defined as the probability that the instantaneous SNR takes a value below a given threshold, γ_{th}. It can be obtained from the CDF (11) as

$$\mathrm{OP} = F_\gamma(\gamma_{\mathrm{th}}). \quad (16)$$

Fig. 3 shows the OP under fSOSF model, for different values of the parameter m. Additional parameters are set to $\alpha = 0.1$ and $\beta = 0.7$, and two threshold values are considered: $\gamma_{\mathrm{th}} = 3$ dB and $\gamma_{\mathrm{th}} = 1$ dB.

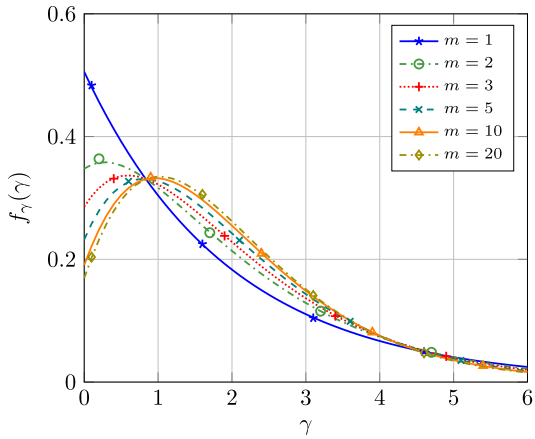

Fig. 1. PDFs of fSOSF model for different values of m. Parameter values are $\alpha = 0.1$, $\beta = 0.7$ and $\overline{\gamma}_{\mathrm{dB}} = 3$ dB. Theoretical values (10) are represented with lines. Markers correspond to MC simulations.

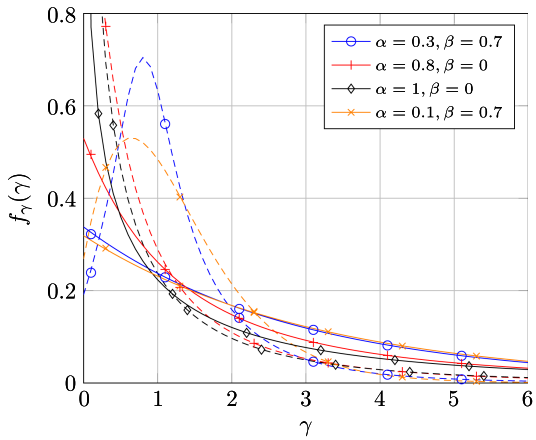

Fig. 2. PDFs comparison for different values of α and β. Solid/dashed lines obtained with (10) correspond to ($m = 1$, $\overline{\gamma}_{\mathrm{dB}} = 5$ dB) and ($m = 20$, $\overline{\gamma}_{\mathrm{dB}} = 1$ dB), respectively. Markers correspond to MC simulations.

$$\mathcal{M}_\gamma^{(n)}(s) = \sum_{q=0}^{n-m} \binom{n}{q} \frac{(-1)^{q+1}(m-n-q)_{n-q}(m)_q}{s^{n+1}\overline{\gamma}\alpha} \sum_{i=0}^{n-q}\sum_{j=0}^{q} \binom{n-q}{i}\binom{q}{j} c^{n-q-i}d^{q-j} \times \left[\sum_{k=1}^{n+1-m-q} A_k(s)\mathrm{U}(k,k,a(s)) + \sum_{k'=1}^{m+q} B_k(s)\mathrm{U}(k',k',b(s))\right] + \sum_{q=n+1-m}^{n} \binom{n}{q} \frac{(-1)^{q+1}(m-n-q)_{n-q}(m)_q}{s^{n+1}\overline{\gamma}\alpha} \sum_{i=0}^{n-q}\sum_{j=0}^{q} \binom{n-q}{i}\binom{q}{j} c^{n-q-i}d^{q-j} \times \sum_{r=0}^{m-1-n+q} \binom{m-1-n+q}{r} a(s)^{m-1-n+q-r}\Gamma(1+r+i+j)\mathrm{U}(m+q, m+q-r-i-j, b(s)). \quad (13)$$

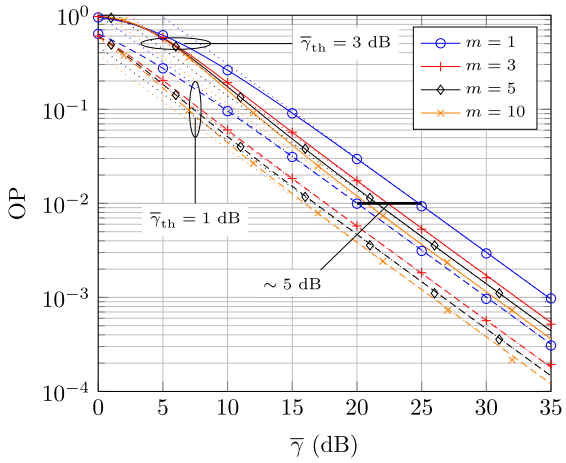

Fig. 3. OP as a function of $\overline{\gamma}$, for different values of m. Parameter values are $\alpha = 0.1$ and $\beta = 0.7$. Solid/dashed lines correspond to $\gamma_{\rm th} = 3$ and $\gamma_{\rm th} = 1$ respectively. Theoretical values (16) are represented with lines. Markers correspond to MC simulations.

We see that a 2 dB change in the threshold SNR is translated into a ~ 5 dB power offset in terms of OP performance. We observe that as the severity of fading increases (i.e., $\downarrow m$), the less likely it is to exceed the threshold value $\gamma_{\rm th}$, i.e., the higher the OP. In all instances, the diversity order (i.e., the down-slope decay of the OP) is one, and the asymptotic OP in (17) tightly approximates the exact OP, being the former given by

$$\mathrm{OP}\left(\alpha,\beta,m;\overline{\gamma},\gamma_{\rm th}\right) \approx \frac{\gamma_{\rm th}}{\alpha\overline{\gamma}} \sum_{j=0}^{m-1} \binom{m-1}{j} \left(\tfrac{1-\beta-\alpha}{\alpha}\right)^{m-1-j} \times \Gamma(1+j)\mathrm{U}\left(m, m-j, \tfrac{1}{\alpha} - \tfrac{\beta}{\alpha}\left(\tfrac{m-1}{m}\right) - 1\right). \tag{17}$$

Expression (17) can be readily derived by integration over the asymptotic OP of the underlying RS model [16, eq. (22)].

V. Conclusion

We presented a generalization of Andersen's SOSF model by incorporating random fluctuations on its dominant specular component, without incurring in additional complexity. Some insights have been provided on how the set of parameters (α, β and m) affect propagation, and its application to performance analysis has been exemplified through an outage probability analysis. A second-order statistical characterization of the family of SOSF models remains an open challenge in the literature, and will likely shed light on the dynamic behavior of fading under these propagation conditions.

Appendix A
Proof of Lemma 1

Noting that $x = |G_3|^2$ is exponentially distributed with unitary mean, we can compute the distribution of γ by averaging over all possible values of x as:

$$f_\gamma(\gamma) = \int_0^\infty f_{\gamma_x}(\gamma; x) e^{-x} dx. \tag{18}$$

The PDFs of γ_x is that of a squared RS RV, which for integer m is given by [19, eq. (5)]

$$f_{\gamma_x}(\gamma; x) = \sum_{j=0}^{m-1} B_j \left(\tfrac{m-j}{\omega_B}\right)^{m-j} \tfrac{\gamma^{m-j-1}}{(m-j-1)!} e^{-\frac{\gamma(m-j)}{\omega_B}}, \tag{19}$$

where

$$B_j = \binom{m-1}{j} \left(\tfrac{m}{K_x+m}\right)^j \left(\tfrac{K_x}{K_x+m}\right)^{m-j-1}, \tag{20}$$

$$\omega_B = (m-j)\left(\tfrac{K_x}{K_x+m}\right)\left(\tfrac{\overline{\gamma}_x}{1+K_x}\right). \tag{21}$$

with K_x and $\overline{\gamma}_x$ given in (7) and (8). Substituting (19) into (18), using the change of variables $t = \frac{1}{\alpha}(1 - \beta(\frac{m-1}{m}) - \alpha(1-x))$ and taking into account that $(t - \frac{\beta}{\alpha m})^j = \sum_{r=0}^{j} \binom{j}{r} t^j (\frac{\beta}{\alpha m})^{j-r}$, the proof is completed.

Appendix B
Proof of Lemma 2

The CDF of the fSOSF model is derived by averaging the CDF of γ_x, i.e., the RS CDF over the exponential distribution:

$$F_\gamma(\gamma) = \int_0^\infty F_{\gamma_x}(\gamma; x) e^{-x} dx. \tag{22}$$

For the case of integer m, a closed-form expression for the RS CDF is presented in [19, eq. (10)], i.e.

$$F_{\gamma_x}(\gamma; x) = 1 - \sum_{j=0}^{m-1} B_j e^{\frac{-\gamma(m-j)}{\omega_B}} \sum_{r=0}^{m-j-1} \tfrac{1}{r!} \left(\tfrac{\gamma(m-j)}{\omega_B}\right)^r, \tag{23}$$

Substituting (23) in (22) and following the same approach used in the previous appendix, the proof is completed.

Appendix C
Proof of Lemma 3

Following the same procedure, the GMGF of the fSOSF model denoted as $\mathcal{M}_\gamma^{(n)}(s)$ can be obtained by averaging the GMGF of γ_x, i.e., the Rician shadowed GMGF over the exponential distribution:

$$\mathcal{M}_\gamma^{(n)}(s) = \int_0^\infty \mathcal{M}_{\gamma_x}^{(n)}(s; x) e^{-x} dx. \tag{24}$$

A closed-form expression for $M_{\gamma_x}(s; x)$ for integer m is provided in [19, eq. (26)]

$$M_{\gamma_x}(s; x) = \tfrac{m^m (1+K_x)}{\overline{\gamma}_x (K_x+m)^m} \tfrac{\left(s - \frac{1+K_x}{\overline{\gamma}_x}\right)^{m-1}}{\left(s - \frac{1+K_x}{\overline{\gamma}_x} \frac{m}{K_x+m}\right)^m} \tag{25}$$

Substituting (7) and (8) into (25), we rewrite

$$M_{\gamma_x}(s; x) = F_1(s; x) \cdot F_2(s; x), \tag{26}$$

where

$$F_1(s; x) = -\left[s\overline{\gamma}\left(1 - \beta - \alpha(1-x)\right) - 1\right]^{m-1}, \tag{27}$$

$$F_2(s; x) = \left[s\overline{\gamma}\left(1 - \beta\left(\tfrac{m-1}{m}\right) - \alpha(1-x)\right) - 1\right]^{-m}. \tag{28}$$

Next, we compute the n-th derivative of (26) which yields the RS GMGF

$$\mathcal{M}_{\gamma_x}^{(n)}(s; x) = \tfrac{\partial^n M_{\gamma_x}(s;x)}{\partial s^n} = \sum_{q=0}^{n} \binom{n}{q} F_1^{(n-q)}(s; x) \cdot F_2^{(q)}(s; x), \tag{29}$$

where $F_i^{(n)}(s; x)$ denotes the n-th derivative of $F_i(s; x)$ with respect to s.

$$F_1^{(n-q)}(s; x) = -(m-n+q)_{n-q} s^{m-1-n+q} (\overline{\gamma}\alpha)^{m-1} \times (x + a(s))^{m-1-n+q} (x+c)^{n-q} \tag{30}$$

$$F_2^{(q)}(s; x) = (-1)^q (m)_q s^{-m-q} (\overline{\gamma}\alpha)^{-m} \times (x + b(s))^{-m-q} (x+d)^q, \tag{31}$$

where $(z)_j$ denotes the Pochhammer symbol and where

$$a(s) = \frac{s\overline{\gamma}(1-\beta-\alpha)-1}{s\overline{\gamma}\alpha}, \tag{32}$$

$$b(s) = \frac{s\overline{\gamma}\left(1-\beta\left(\frac{m-1}{m}\right)-\alpha\right)-1}{s\overline{\gamma}\alpha}, \tag{33}$$

$$c = \frac{1-\beta}{\alpha} - 1, \tag{34}$$

$$d = \frac{1-\beta\left(\frac{m-1}{m}\right)}{\alpha} - 1. \tag{35}$$

From (29), (30) and (31) notice that $\mathcal{M}_{\gamma_x}^{(n)}(s;x)$ is a rational function of x with two real positive zeros at $x=c$ and $x=d$, one real positive pole at $x=b(s)$ and one real positive zero or pole at $x=a(s)$ depending on whether $m \geq n+1$ or not. Integration of (24) is feasible with the help of [20, eq. 13.4.4]

$$\int_0^\infty \frac{x^i}{(x+p)^j} e^{-x} dx = \Gamma(i+1)\mathrm{U}(j, j-i, p). \tag{36}$$

where $\mathrm{U}(\cdot,\cdot,\cdot)$ is Tricomi's confluent hypergeometric function. We need to expand $\mathcal{M}_{\gamma_x}^{(n)}(s;x)$ in partial fractions of the form $\frac{x^i}{(x+p)^j}$. Two cases must be considered:

- $m \geq n+1$
  In this case there is only one pole at $x=b(s)$ and no partial fraction expansion is required. Using the fact that $(x+p)^n = \sum_{i=0}^n x^i p^{n-i}$, then (12) is obtained.
- $m < n+1$
  Now, there are two poles ($x=a(s)$, $x=b(s)$). After performing partial fraction expansion we obtain (13).

Appendix D
Proof of Lemma 4

Using the definition of γ_x, we can write

$$\mathbb{E}[\gamma^n] = \int_0^\infty \mathbb{E}[\gamma_x^n] e^{-x} dx. \tag{37}$$

where $\mathbb{E}[\gamma_x^n] = \lim_{s\to 0^-} M_{\gamma_x}^{(n)}(s;x)$ where $M_{\gamma_x}^{(n)}(s;x)$ is given in (29). Performing the limit and using the integral $\int_0^\infty x^p e^{-x} dx = p!$, the proof is complete.

References

[1] P. S. Bithas, K. Maliatsos, and A. G. Kanatas, "The bivariate double Rayleigh distribution for multichannel time-varying systems," *IEEE Wireless Commun. Lett.*, vol. 5, no. 5, pp. 524–527, Oct. 2016.

[2] Y. Ai, M. Cheffena, A. Mathur, and H. Lei, "On physical layer security of double Rayleigh fading channels for vehicular communications," *IEEE Wireless Commun. Lett.*, vol. 7, no. 6, pp. 1038–1041, Dec. 2018.

[3] P. S. Bithas, A. G. Kanatas, D. B. da Costa, P. K. Upadhyay, and U. S. Dias, "On the double-generalized gamma statistics and their application to the performance analysis of V2V communications," *IEEE Trans. Commun.*, vol. 66, no. 1, pp. 448–460, Jan. 2018.

[4] P. S. Bithas, V. Nikolaidis, A. G. Kanatas, and G. K. Karagiannidis, "UAV-to-ground communications: Channel modeling and UAV selection," *IEEE Trans. Commun.*, vol. 68, no. 8, pp. 5135–5144, Aug. 2020.

[5] J. K. Devineni and H. S. Dhillon, "Ambient backscatter systems: Exact average bit error rate under fading channels," *IEEE Trans. Green Commun. Netw.*, vol. 3, no. 1, pp. 11–25, Mar. 2019.

[6] U. Fernandez-Plazaola, L. Moreno-Pozas, F. J. Lopez-Martinez, J. F. Paris, E. Martos-Naya, and J. M. Romero-Jerez, "A tractable product channel model for line-of-sight scenarios," *IEEE Trans. Wireless Commun.*, vol. 19, no. 3, pp. 2107–2121, Mar. 2020.

[7] E. Vinogradov, W. Joseph, and C. Oestges, "Measurement-based modeling of time-variant fading statistics in indoor peer-to-peer scenarios," *IEEE Trans. Antennas Propag.*, vol. 63, no. 5, pp. 2252–2263, May 2015.

[8] V. Nikolaidis, N. Moraitis, P. S. Bithas, and A. G. Kanatas, "Multiple scattering modeling for dual-polarized MIMO land mobile satellite channels," *IEEE Trans. Antennas Propag.*, vol. 66, no. 10, pp. 5657–5661, Oct. 2018.

[9] J. B. Andersen, "Statistical distributions in mobile communications using multiple scattering," in *Proc. 27th URSI Gen. Assem.*, 2002, pp. 1–4.

[10] J. Salo, H. M. El-Sallabi, and P. Vainikainen, "Statistical analysis of the multiple scattering radio channel," *IEEE Trans. Antennas Propag.*, vol. 54, no. 11, pp. 3114–3124, Nov. 2006.

[11] J. Lopez-Fernandez and F. J. Lopez-Martinez, "Statistical characterization of second-order scattering fading channels," *IEEE Trans. Veh. Technol.*, vol. 67, no. 12, pp. 11345–11353, Dec. 2018.

[12] A. Abdi, W. C. Lau, M. Alouini, and M. Kaveh, "A new simple model for land mobile satellite channels: First- and second-order statistics," *IEEE Trans. Wireless Commun.*, vol. 2, no. 3, pp. 519–528, May 2003.

[13] J. F. Paris, "Statistical characterization of $\kappa-\mu$ shadowed fading," *IEEE Trans. Veh. Technol*, vol. 63, no. 2, pp. 518–526, Feb. 2014.

[14] J. M. Romero-Jerez, F. J. Lopez-Martinez, J. P. Peña-Martín, and A. Abdi, "Stochastic fading channel models with multiple dominant specular components," *IEEE Trans. Veh. Technol.*, vol. 71, no. 3, pp. 2229–2239, Mar. 2022.

[15] J. M. Romero-Jerez, F. J. Lopez-Martinez, J. F. Paris, and A. J. Goldsmith, "The fluctuating two-ray fading model: Statistical characterization and performance analysis," *IEEE Trans. Wireless Commun.*, vol. 16, no. 7, pp. 4420–4432, Jul. 2017.

[16] J. López-Fernández, P. Ramirez-Espinosa, J. M. Romero-Jerez, and F. J. López-Martínez, "A fluctuating line-of-sight fading model with double-Rayleigh diffuse scattering," *IEEE Trans. Veh. Technol.*, vol. 71, no. 1, pp. 1000–1003, Jan. 2022.

[17] M. Chaudhry and S. Zubair, "Generalized incomplete gamma functions with applications," *J. Comput. Appl. Math.*, vol. 55, no. 1, pp. 99–123, 1994.

[18] L. Moreno-Pozas, F. J. Lopez-Martinez, J. F. Paris, and E. Martos-Naya, "The $\kappa-\mu$ Shadowed Fading Model: Unifying the $\kappa-\mu$ and $\eta-\mu$ distributions," *IEEE Trans. Veh. Technol.*, vol. 65, no. 12, pp. 9630–9641, Dec. 2016.

[19] F. J. Lopez-Martinez, J. F. Paris, and J. M. Romero-Jerez, "The κ-μ shadowed fading model with integer fading parameters," *IEEE Trans. Veh. Technol*, vol. 66, no. 9, pp. 7653–7662, Sep. 2017.

[20] F. W. J. Olver et al., "NIST digital library of mathematical functions," Release 1.0.21 of 2018-12-15. [Online]. Available: http://dlmf.nist.gov/